Water Diffusion Proceeds via a Hydrogen-Bond Jump Exchange Mechanism

Axel Gomez, Zeke A Piskulich, Ward Thompson, Damien Laage

Water Diffusion Proceeds via a Hydrogen-Bond Jump Exchange Mechanism

Axel Gomez,[†] Zeke A. Piskulich,[‡,¶] Ward H. Thompson,[*,‡] and Damien Laage[*,†]

†*PASTEUR, Department of Chemistry, École normale supérieure, PSL University, Sorbonne Université, CNRS, 75005 Paris, France*

‡*Department of Chemistry, University of Kansas, Lawrence, Kansas 66045, USA*

¶*Present address: Department of Chemistry, Boston University, Boston, MA 02215 USA*

E-mail: wthompson@ku.edu; damien.laage@ens.psl.eu

Abstract

The self-diffusion of water molecules plays a key part in a broad range of essential processes in biochemistry, medical imaging, material science and engineering. However, its molecular mechanism and the role played by the water hydrogen-bond network rearrangements are not known. Here we combine molecular dynamics simulations and analytic modeling to determine the molecular mechanism of water diffusion. We establish a quantitative connection between the water diffusion coefficient and hydrogen-bond jump exchanges, and identify the features that determine the underlying energetic barrier. We thus provide a unified framework to understand the coupling between translational, rotational, and hydrogen-bond dynamics in liquid water. It explains why these different dynamics do not necessarily exhibit identical temperature dependences although they all result from the same hydrogen-bond exchange events. The consequences for the understanding of water diffusion in supercooled conditions and for water transport in complex aqueous systems, including ionic, biological, and confined solutions are discussed.

Graphical TOC Entry

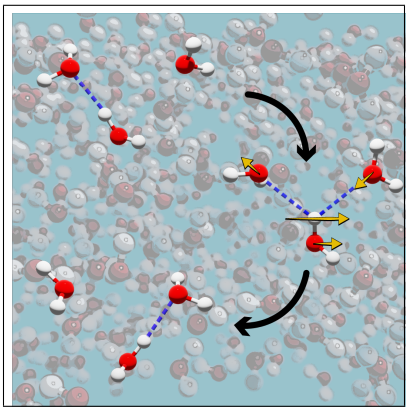

Characterizing and manipulating the diffusion of water is a major challenge for a broad range of processes and systems, including, *e.g.*, fuell cell membranes,[1] cryopreservation of biomolecules,[2] protection against corrosion,[3] and biomedical imaging of brain stroke and cancer.[4] However, a molecular picture of the mechanism that governs how water molecules move through the liquid and of the energetic barrier that determines the diffusion coefficient has remained elusive. A distinctive feature of water is the extended hydrogen-bond (H-bond) network that permeates the liquid.[5,6] Since each water molecule is connected to its nearest neighbors by H-bonds, any displacement beyond the molecular cage is expected to require a rearrangement of the H-bond network. However, while H-bond exchanges have been shown to be responsible for water reorientation,[7,8] such a connection has been missing for translational dynamics, despite the great importance that identifying the molecular translational diffusion mechanism would have for an improved understanding of water transport properties.

Water diffusion has often been described with random walk and jump diffusion models involving elementary hops.[9–11] However, these models have only been used as effective descriptions, and the molecular mechanism of these elementary hops and their connection with H-bond rearrangements have not been characterized. In addition, the molecular parameters obtained from these effective models were often not consistent with other dynamical studies: for example, the inferred delays between successive hops[9–11] did not match any known timescale for the H-bond network dynamics. In the absence of a characterization of the elementary events that would justify a jump diffusion description, it has also been suggested[6,12] that a continuous model would be preferable.

Here we establish an explicit connection between H-bond network rearrangements and molecular translational diffusion in liquid water. We use molecular dynamics (MD) simulations to characterize the mechanism that governs the translational displacements induced by H-bond exchanges, and show how an extended jump diffusion model provides an excellent description of water diffusion dynamics. We identify the molecular contributions to the diffusion energetic barrier, and explain why translational and rotational water dynamics,

although they proceed from the same H-bond exchanges, exhibit slightly different temperature dependences. We finally discuss the consequences for water dynamics in complex environments.

To elucidate the impact of H-bond rearrangements on water translational dynamics, our starting point lies in the characterization of elementary H-bond exchange events that govern every change in the H-bond network connectivity. An H-bond exchange occurs when a water OH group switches H-bond acceptors,[7,8] and its mechanism has been shown via simulations to proceed through large-amplitude angular jumps, which cause the H-bond donating OH group to reorient[7,8] (Fig. 1a). Jump H-bond exchanges have been found in a wide range of aqueous systems,[8] and have been characterized by nonlinear vibrational spectroscopy experiments in aqueous salt solutions.[13,14] Because their mechanism involves the elongation and contraction of the H-bonds being broken and formed,[7,8] they are expected to induce translational displacements of the water partners, and prior simulations[15,16] showed that molecules that experience these jumps tend to diffuse faster. However, the precise impact of these jumps on the H-bond donor and acceptors' translational dynamics has thus far not been determined.

Prior works have established that classical MD simulations are a particularly incisive tool to investigate water H-bond exchanges.[7,8] Our present study employs classical MD simulations on liquid water at 298.15 K and the equilibrium density found at 1 atm (see SI for details). In the following, we present results obtained with the TIP4P/2005 potential,[17] which provides a very good description of water dynamics and of its temperature dependence.[17,18] Complementary results obtained with the SPC/E force field[19] are also reported and show that our model is robust vis-a-vis the choice of water potential.

To determine the translational displacements associated with H-bond exchanges in our molecular dynamics trajectory, we consider all the events where a water OH group (noted O^*H^* in the following) switches from an initial acceptor O_i to form a new H-bond with a different acceptor O_f. Strict geometric H-bond criteria ($R_{OO} < 3.1$ Å and $\theta_{HOO} < 15°$) are

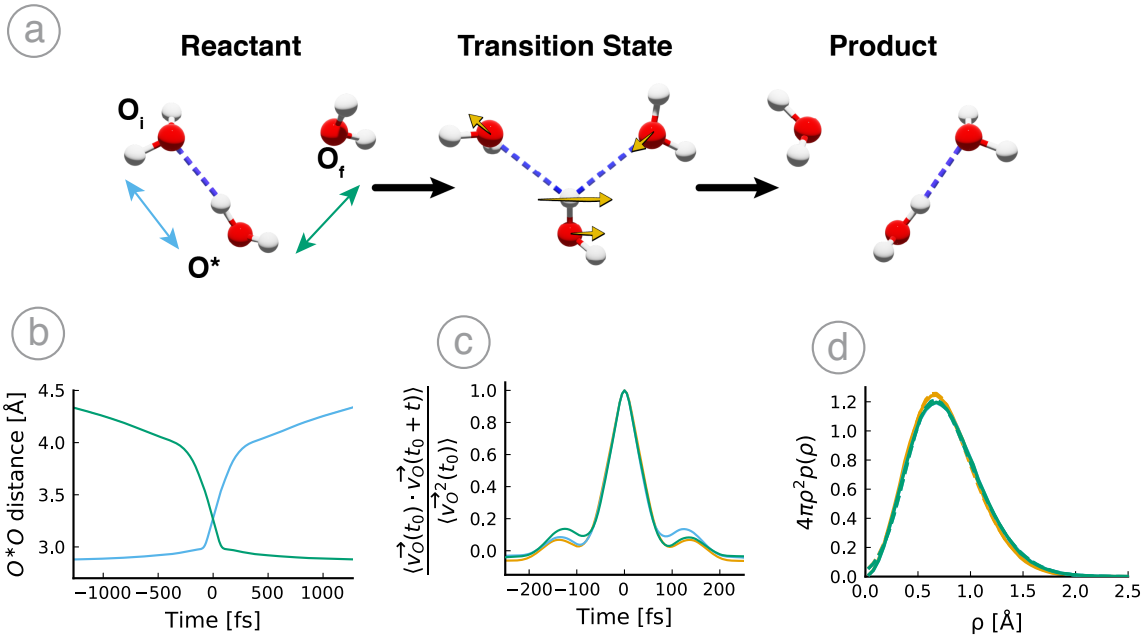

Figure 1: Hydrogen-bond jump exchange mechanism and translational displacement. a) Schematic representation of H-bond exchange mechanism, with average displacement vector orientations for each molecule (yellow). b) Time evolution of the average O^*O_i (blue) and O^*O_f (green) distances. c) Velocity time-correlation functions for the O^* (orange), O_i (blue) and O_f (green) oxygen atoms. d) Jump amplitude probability densities $4\pi\rho^2 p(\rho)$ for the O^* (orange), O_i (blue) and O_f (green) oxygen atoms, and skew normal fits (dashes) (see Table S2 for fit parameters).

employed to focus on exchanges between stable H-bonds. For each exchange, the transition state crossing is defined to be the instant t_0 when the O^*H^* group crosses the bisector plane between the initial and final acceptors with the largest angular velocity. Trajectories before and after t_0 are collected as long as neither the O^*H^* group nor any of the parent water molecule's other H-bonds experience another stable exchange; this ensures that the impact of a single exchange is considered. Averages are then calculated over the collection of exchange events.

Figure 1b shows that the breaking of the initial H-bond with O_i and the formation of the new bond with O_f lead to the elongation and contraction of the O^*O_i and O^*O_f distances, respectively. H-bond exchanges thus induce translational displacements of the water molecules involved and we now determine their respective amplitudes in the laboratory

frame. In contrast to OH reorientation which occurs between stable orientations defined by the initial and final H-bond acceptor positions,[7,8] there is no stable position for the water oxygen that can be easily defined, *e.g.*, based on the surrounding hydration shell configuration. We therefore calculate the oxygen velocity time-correlation function $C_{vv}(t) = \langle \overrightarrow{v_O}(t_0) \cdot \overrightarrow{v_O}(t_0 + t) \rangle$ and use the time when it reaches its first minimum before or after t_0 as an approximate determination of the delay required for the oxygen to reach its stable position. Figure 1c presents C_{vv} for the H-bond donor oxygen O^*, and the initial O_i and final O_f H-bond acceptors, and shows that a stable position is reached for a delay $\Delta t \simeq$100 fs after the exchange transition state is crossed. We therefore determine the translational jump displacement of each oxygen atom as the vector connecting the positions before and after the H-bond exchange $\overrightarrow{\rho} = \overrightarrow{r_O}(t_0 + \Delta t) - \overrightarrow{r_O}(t_0 - \Delta t)$.

For the three water oxygen atoms involved in the H-bond exchange, jump amplitude probability density distributions $4\pi\rho^2 p(\rho)$ are reported in Fig. 1d. They are all well described by skew normal distributions, with a peak at $\simeq$0.6-0.7 Å and a tail extending to larger amplitudes. Time reversibility requires that the O_i and O_f distributions be strictly identical. In addition, our results find only minor differences between the O^*O_i and O^*O_f donor-acceptor distributions, with the former exhibiting a slightly broader tail. The resulting average squared amplitudes are thus fairly similar $\langle \rho^2_{O^*} \rangle$=0.675±0.003 Å^2 and $\langle \rho^2_{O_{i,f}} \rangle$=0.722±0.002 Å^2. (All reported uncertainties correspond to the Student's t-distribution 95% confidence interval.) It is interesting to note that the sum of the donor and acceptor root-mean-squared jump amplitudes $\sqrt{\langle \rho^2_{O^*} \rangle} + \sqrt{\langle \rho^2_{O_{i,f}} \rangle} \simeq$1.7 Å is almost equal to the distance between the first ($\simeq$2.8 Å) and second ($\simeq$ 4.5 Å) shell peak positions in the oxygen–oxygen radial distribution function. The average jump vectors for each water partner are schematically shown in Figure 1a and given in Table S1. Their orientations are not isotropically distributed in the local molecular frame: the average O^* displacement lies in the $O^*O_iO_f$ plane and is parallel to the O_iO_f axis. The O_i and O_f partners move away from and toward O^*, respectively. The displacements of the three partners are thus evocative of a reaction coordinate at the transition state that is

an antisymmetric vibrational mode, even if the trimer cannot be considered as an isolated system because of the surrounding liquid.

H-bond jump exchange dynamics are characterized by the jump time-correlation function (tcf) $1 - \langle p_i(0)p_f(t)\rangle$ where p_i (resp. p_f) is 1 when the O^*H^* group forms a stable H-bond with O_i (resp. O_f) and 0 otherwise.[20] Absorbing boundary conditions in the product state ensure that only a single H-bond exchange is considered. The jump tcf exhibits a single exponential decay (see SI Appendix Fig. S1) which suggests that jumps are well described by a Poisson process at ambient conditions. The H-bond jump time (inverse rate) is defined as[20]

$$\tau_{HB} = \int_0^\infty \mathrm{d}t \ \left[1 - \langle p_i(0)p_f(t)\rangle\right] \tag{1}$$

and is calculated to be τ_{HB}=3.657±0.007 ps.[18]

Each water molecule is involved in successive H-bond exchanges, either as an H-bond donor via one of its two hydrogen atoms, or as an acceptor via its oxygen atom. To connect these exchanges to the resulting diffusive motion, we use the continuous time random walk (CTRW) model,[21] which generalizes the discrete random walk model to a continuous distribution from which waiting times between successive hops are randomly drawn. For simplicity, we consider that successive jumps on the same water molecule are independent, and adopt the CTRW form adapted to a single Poisson process. The water diffusion coefficient due to H-bond exchanges directly involving the molecule that diffuses is therefore the sum of independent CTRW contributions from the two H-bond donating hydrogen atoms and the two H-bond accepting sites on the oxygen atom (because we consider only stable H-bond exchanges, transient under- and over-coordination events do not need to be considered),

$$D_{HB} = D_{don} + D_{acc} = 2\frac{\langle \rho^2_{O^*}\rangle}{6\tau_{HB}} + 2\frac{\langle \rho^2_{O_{i,f}}\rangle}{6\tau_{HB}} = \frac{\langle \rho^2_{O^*}\rangle + \langle \rho^2_{O_{i,f}}\rangle}{3\ \tau_{HB}}\ , \tag{2}$$

and at 298.15 K our simulations yield $D_{HB} = (1.273 \pm 0.004) \times 10^{-5}\ \mathrm{cm^2 \cdot s^{-1}}$ (see Table S3).

However, water molecules are not necessarily immobile while they keep their H-bonds

with their nearest neighbors intact. For reorientation, it has been shown[7,8] that an intact H-bonded pair of water molecules can tumble in the liquid, thus reorienting the local frame between successive H-bond jump exchanges and bringing a (minor) contribution to the overall reorientation. In a similar fashion, we determine the translational diffusion coefficient for a water molecule surrounded by the same four nearest neighbors. To circumvent the difficulty caused by the very short lifetime of such an intact cluster, we apply soft restraints between the central water molecule and each of its four neighbors (see SI Appendix), so that these H-bonds can transiently break but no stable exchange can occur. These restraints – which do not significantly perturb the local structure (see SI Appendix Fig. S2) – are key to calculating the $H_2O(H_2O)_4$ complex mean square displacement (msd) at long delays. The latter are essential to reach the diffusive regime visible in Fig. 2 and correctly determine the diffusion coefficient (without such restraints, a prior study[15] could only access the intact cluster msd at shorter delays where the msd appears sub-diffusive). Figure 2 compares the msd of a single water molecule and of a molecule which keeps its four nearest neighbors. A molecule that does not undergo any H-bond exchange with one of its four neighbors diffuses approximately four times more slowly than an average molecule (see Table S3). This frame diffusion component that takes place between successive H-bond exchanges is thus small but non-negligible, and since frame diffusion and H-bond exchanges are statistically independent translational displacement sources, the overall diffusion coefficient results from the sum of the respective diffusion coefficients.

Frame diffusion presumably must arise from H-bond exchanges taking place at the interface between the $H_2O(H_2O)_4$ complex and the rest of the liquid; a CTRW modeling of the latter would be expected to involve the same τ_{HB} jump time but now affecting a larger number of H-bonds resulting in smaller amplitude displacements of the central water molecule. The value of the $H_2O(H_2O)_4$ msd at short times, before the diffusive regime is established, can be used to estimate the amplitude of the fast molecular position fluctuations while the hydration shell is intact. Figure 2 shows that this amplitude is $\simeq 0.7$ Å, which is thus of the

same order as the amplitude of translational jumps induced by H-bond exchanges (Fig. 1d). The overlap between fast local fluctuations and jump displacement amplitudes explains why a visual inspection of the trajectory[6] does not easily reveal sudden discrete hops that are typically expected in a jump diffusion process.

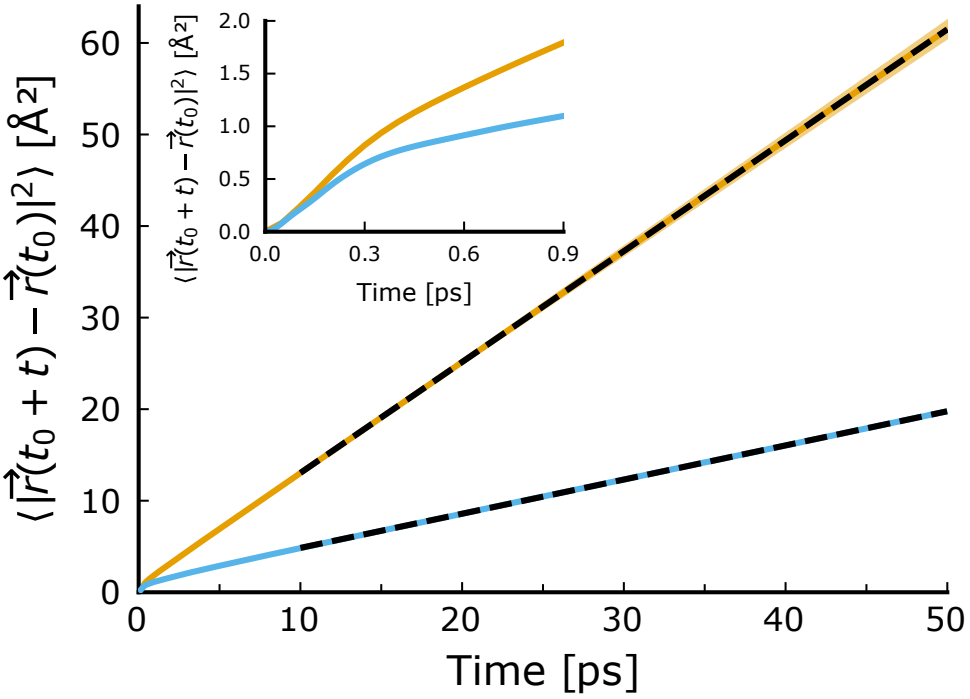

Figure 2: Mean square displacement of a single molecule (orange) and of a molecule keeping the same four H-bonded neighbors (blue), with their short-time behavior shown in the inset. $D_{\mathrm{MD}}^{\mathrm{pbc}}$ and $D_{\mathrm{frame}}^{\mathrm{pbc}}$ are determined from the slopes of linear regressions (dashes) on the 10–50 ps interval.

Our simulations are performed in finite-size boxes which are periodically replicated, and an additional hydrodynamic correction due to the periodic boundary conditions (pbc)[22,23] should be included for comparisons with experimental values,

$$D_{\mathrm{corr}} = \frac{k_B T \zeta}{6\pi\eta L} \tag{3}$$

where T is the system temperature, η the shear viscosity, L the cubic simulation box side and $\zeta \simeq 2.837297$. The shear viscosity was determined from the time integral of the pressure tensor time-correlation function, calculated from a separate set of simulations performed on

the same system (see SI Appendix).

We can now express the overall diffusion coefficient as the sum of the diffusion coefficients coming from *i)* H-bond exchanges involving the central water molecule, *ii)* the local frame diffusion due to H-bond exchanges further away, and *iii)* the pbc correction:

$$D_{\text{model}} = D^{\text{pbc}}_{\text{model}} + D_{\text{corr}} = \left(D_{\text{HB}} + D^{\text{pbc}}_{\text{frame}}\right) + D_{\text{corr}} \tag{4}$$

The resulting $D_{\text{model}} = (2.232 \pm 0.006) \times 10^{-5}\text{cm}^2 \cdot \text{s}^{-1}$ value is in excellent agreement with the experimental value $D_{\text{NMR}} = 2.299 \times 10^{-5}\text{cm}^2 \cdot \text{s}^{-1}$ measured[24,25] by NMR at 298.15 K. Even more importantly to assess the validity of our translational jump model, the agreement is also excellent between our model prediction and the value directly determined from the simulated mean-square displacement of a single water molecule and corrected for pbc, $D_{MD} = D^{pbc}_{MD} + D_{corr} = (2.37 \pm 0.01) \times 10^{-5}$ cm$^2 \cdot$ s^{-1}. In addition, this very good agreement between model and simulations is obtained for both TIP4P/2005 and SPC/E force fields, as graphically summarized in Fig. 3a and detailed in Table S3. These results show that our jump model provides a quantitative description of water translational diffusion, and reveal that H-bond jump exchanges bring the major contribution to the overall translational diffusion. Because H-bond jumps go through a 5-coordinate transition-state, our results thus explain why prior simulations[26] had observed that overcoordinated water molecules tend to diffuse faster, but our model also stresses that such configurations are unstable.

The picture that emerges from this extended jump model for water translational dynamics is that diffusion primarily derives from H-bond exchanges involving the water molecule either as an H-bond donor or as an acceptor, with a minor but non-negligible contribution due to the local frame diffusion between successive H-bond exchanges.

We now briefly contrast this picture with prior jump descriptions of water translational diffusion. Prior studies[10,11,16,27] considered that water structural dynamics could be separated into a fast rattling motion within a local basin, for example formed by the surrounding

water molecules in the cage model,[27] and slower inter-basin jumps. However, our results in Fig. 2 show that water molecules continue to diffuse even when their four H-bond neighbors are unchanged, so that a separation into different mechanisms based on the displacement amplitude is not adequate. The approaches used in these prior studies have faced several limitations. For example, structural clustering based on a 0.7 Å minimum distance between local basins[10] ignored small-amplitude jumps (shown to be important in Fig. 1d) and consequently led to an overestimated ≃3 ps jump time at 297.1 K,[10] which is surprisingly long since it is close to the H-bond exchange time for a single OH group, while the ∼ 4 H-bond partners of a given molecule would be expected to lead to four times more frequent jumps for the central oxygen. A cage-jump model was independently proposed,[11] where translational jumps occur only once all 4 H-bonds of a molecule break; this is in contrast to our results which show that a water molecule undergoes a translational jump as soon as any one of its 4 H-bonds is exchanged. Consequently this assumption leads to long (≃10 ps) resting periods between successive translational jumps, not seen in molecular dynamics trajectories. A key advantage of our present study is that we identify the elementary jumps directly from H-bonds exchanges, and thus avoid the limitations due to coarse-graining and arbitrary thresholds used in these prior works.

Experimentally, jump models have been used to analyze water QENS spectra,[9,10,28–31] and translational jump time values close to the values obtained here have been shown to be consistent with experimental linewidths.[30] However, QENS spectra probe displacements of water H atoms[28] and, while the latter share the same diffusion coefficient as water O atoms, their motions result from the combination of larger-amplitude jumps when the H atom exchanges H-bond acceptors and smaller-amplitude jumps when the parent O atom experiences an H-bond exchange which does not involve this H. A specific translational jump model for water H atoms combining these two types of exchanges would thus provide a way to model QENS spectra without having to use the traditional but questionable translation-rotation decoupling approximation.[30]

We now examine the temperature dependence predicted by our jump model for the diffusion coefficient and consider the activation energy,

$$E_a^D = k_B T^2 \frac{\partial \ln D}{\partial T} \tag{5}$$

Our motivation is twofold. First, this will assess whether our model can successfully describe water diffusion over a broad range of temperatures. Second, since the activation energy for a chemical reaction can be interpreted[32,33] as the difference in average internal energy between the reacting species and the reactants, we will use the molecular insight given by E_a^D to identify the origin of the underlying energetic barrier to diffusion.

The activation energy is traditionally obtained from a numerical temperature derivative calculated via an Arrhenius plot constructed from measurements (or simulations) at multiple temperatures. In contrast, here we use the recently-introduced fluctuation theory for dynamics method[33,34] that directly determines E_a from the analytic temperature derivative calculated from a single simulation. This presents several advantages: it requires only simulations at a single temperature, it avoids ambiguities due to the choice of temperature range for non-Arrhenius processes analyzed with the traditional approach, and it reveals which interactions contribute to the activation energy.

The activation energy predicted by our jump model is obtained by combining eqs 4 and 5. The activation energy of the pbc-corrected diffusion coefficient is

$$E_a^{D_{model}} = \frac{D_{HB}}{D_{model}^{pbc}} E_a^{D_{HB}} + \frac{D_{frame}^{pbc}}{D_{model}^{pbc}} E_a^{D_{frame}^{pbc}} + \frac{D_{corr}}{D_{model}} \left(E_a^{D_{corr}} - E_a^{D_{model}^{pbc}} \right) \tag{6}$$

The diffusion $E_a^{D_{model}}$ is a weighted average of the H-bond exchange, frame diffusion, and pbc correction activation energies. Using eq. 2, $E_a^{D_{HB}}$ can be further decomposed into terms due to the H-bond jump time and jump amplitude temperature dependence,

$$E_a^{D_{HB}} = E_a^{1/\tau_{HB}} + E_a^{\langle \rho^2 \rangle} = E_a^{1/\tau_{HB}} + \frac{\langle \rho_{O^*}^2 \rangle}{\langle \rho_{O^*}^2 \rangle + \langle \rho_{O_{i,f}}^2 \rangle} E_a^{\langle \rho_{O^*}^2 \rangle} + \frac{\langle \rho_{O_{i,f}}^2 \rangle}{\langle \rho_{O^*}^2 \rangle + \langle \rho_{O_{i,f}}^2 \rangle} E_a^{\langle \rho_{O_{i,f}}^2 \rangle} \tag{7}$$

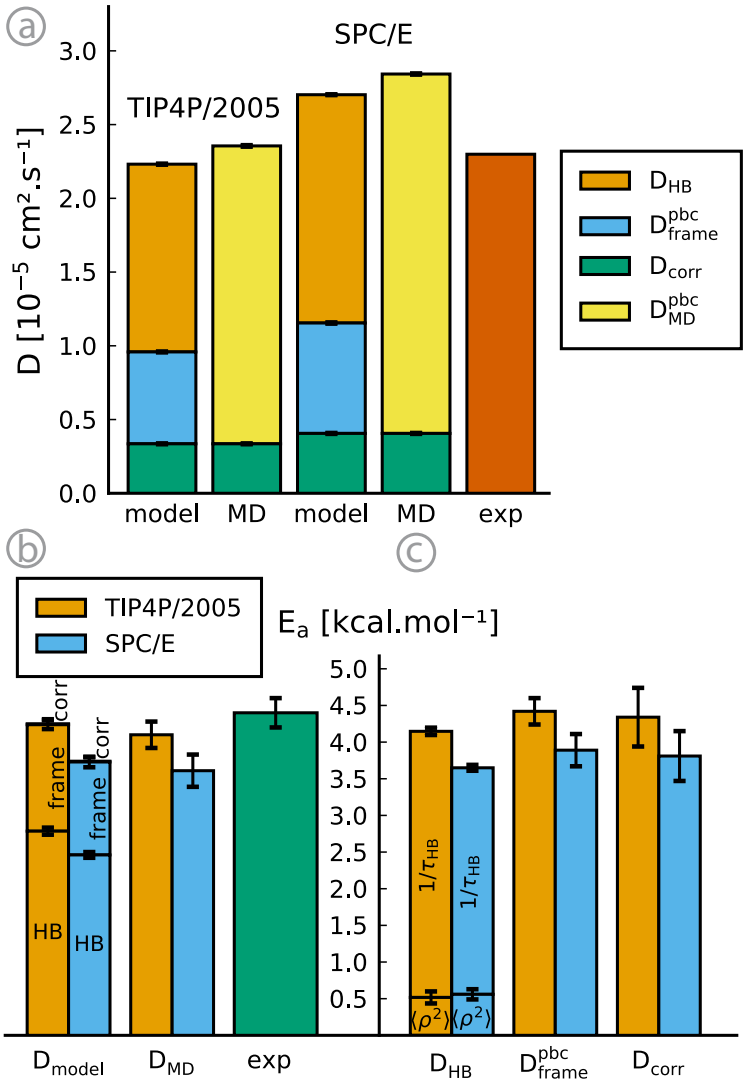

Figure 3: a) Diffusion coefficients from the model eq. 4, from our simulated mean-square displacement and from experiments,[24,25] together with the contributions determined from the jump model, obtained from our TIP4P/2005 and SPC/E simulations (see Table S3). b) Activation energies for the model diffusion coefficient $E_a^{D_{\text{model}}}$ eq. 6 (showing the weight of each contribution in the sum), for the simulated diffusion coefficient $E_a^{D_{\text{MD}}}$ and from experiments[24,25] $E_a^{D_{\text{exp}}}$ and c) for each model contribution $E_a^{D_{\text{HB}}}$, $E_a^{D_{\text{frame}}^{\text{pbc}}}$, $E_a^{D_{\text{corr}}}$.

The respective contributions to the jump model diffusion coefficient activation energy are reported in Fig. 3b-c and Table S3 for both TIP4P/2005 and SPC/E water force fields (see SI for calculations of activation energies in eqs. 6-7). A first important result is that, for both water models, the jump model diffusion activation energy is in excellent agreement with the simulated value (Fig. 3b) which shows that the model provides an accurate description of the

diffusion coefficient over a range of temperatures around ambient conditions and provides further support to the jump model validity.

These results thus suggest that the jump model can be used to gain a molecular insight into the molecular origin of the energetic barrier to diffusion. First, eq. 6 and the values in Fig. 3b-c and Table S3 show that the dominant contribution to $E_a^{D_{model}}$ comes from the H-bond exchange $E_a^{D_{HB}}$ term because these exchanges provide the fastest diffusion pathway, while the pbc correction term is almost negligible because of the very similar values of $E_a^{D_{corr}}$ and $E_a^{D_{model}^{pbc}}$. Second, while $E_a^{D_{model}}$ is very close to the activation energy of the H-bond jump exchange diffusion term $E_a^{D_{HB}}$, $E_a^{D_{model}}$ is notably greater than the H-bond jump exchange rate $E_a^{1/\tau_{HB}}$ (see Table S3) because of the additional $E_a^{\langle\rho^2\rangle}$ term in eq. 7 coming from the increase in translational jump amplitude with increasing temperature.

In addition, the model offers an interpretation to the difference between diffusion and reciprocal viscosity activation energies.[35] The latter contrasts with the expectation from the Stokes-Einstein equation and has been abundantly discussed, especially in the supercooled liquid (see, *e.g.*, refs [36–38]). While the hydrodynamic approximation involved in the Stokes-Einstein equation is questionable for the diffusion of a solute particle that has the same size as the solvent particles, one can expect H-bond jump exchanges to play an important role for both diffusion and viscosity. Eyring and coworkers[39] proposed a simplified picture describing viscosity as an activated process involving displacements between equilibrium positions in the liquid, and simulations suggested[35,40] that H-bond jump exchanges could be these elementary events. Our model suggests that while the same H-bond jump exchanges are involved in diffusion and shear viscosity, any difference in activation energies between D and $1/\eta$ arises from the different temperature dependences of the impact that each jump has on the molecular position and on the stress tensor.

The present results also provide new insight into the coupling between rotational and translational dynamics in water, of particular interest in the supercooled regime.[41–45] The role of H-bond jumps for translation elucidated here can be compared with the extended

angular jump model for reorientation.[7,8] While this rotation-translation coupling is often viewed through the lens of the Debye-Stokes-Einstein equation,[43,44] our model avoids the hydrodynamic approximation, which is not appropriate for a small solute, and the assumption of rotational diffusion for water reorientation, which was shown to be invalid.[7,8] H-bond jump exchanges are central to both rotational and translational dynamics (including at supercooled temperatures[46]), and the jump models indicate that the slight difference between the reorientation time τ_2 and translational diffusion D activation energies arises from the larger temperature dependence of the translational jump amplitude compared to that of the rotational amplitude.[47] This suggests an alternative explanation for why $D \times \tau_2$ increasingly deviates from its ambient temperature value upon supercooling,[48,49] based on differences in the temperature dependences of the translational and rotational jump amplitudes. In contrast to prior suggestions,[50] such a mechanism would thus require neither a decoupling between rotational and translational motion nor a change in diffusion mechanism.

Finally, our results also pave the way to an improved understanding of water transport properties in aqueous solutions and at interfaces. Since our model reveals the connection between the diffusion coefficient and the H-bond jump time and amplitude, the solute's or interface's impact on the latter will be of great importance. The H-bond jump time has been shown in prior studies[8] to sensitively depend on the water-solute or water-surface H-bond interaction strength. Regarding the H-bond amplitude, it is expected to depend on the relative masses of the water molecule and of its H-bond partner. This should provide a framework to understand how water diffusion is affected in electrolytes, including, *e.g.*, the diffusion enhancement and reduction induced by different salts,[51] but also in materials and in biomolecular hydration shells where it should provide a connection between the H-bond jump time heterogeneity[52] and variations in the water diffusion coefficient.

In conclusion, we have described an H-bond jump model for translational dynamics of water that quantitatively describes the water diffusion coefficient and its activation energy. We have shown that translational diffusion of a water molecule is mainly due to jumps

which take place when this molecule exchanges H-bond partners, with a minor contribution from diffusion of molecules that keep their H-bonds intact. Our model thus provides a unified framework which establishes how H-bond network rearrangements are responsible for both translational and rotational dynamics in liquid water. Our analysis of the activation energies further reveals why translation and reorientation activation energies slightly differ, leading to an apparent decoupling while they proceed from the same H-bond exchanges. The molecular insight provided by the jump model for translation dynamics will be instrumental to understand how water transport properties are impacted in more complex environments.

Acknowledgement

Silvio Pipolo (now Univ. Lille, France) is gratefully acknowledged for preliminary work. This work was supported by the National Science Foundation under Grant No. CHE-2102656 (W.H.T.). Z.A.P gratefully acknowledges a National Science Foundation Graduate Research Fellowship under Grant Nos. 1540502 and 1451148 and the Graduate Research Opportunities Worldwide program. Activation energy calculations were performed at the Center for Research Computing (CRC), University of Kansas.

Supporting Information Available

The following files are available free of charge. Simulation methodology, jump displacements, $H_2O(H_2O)_4$ complex diffusion, activation energy and viscosity calculations.

References

(1) Tsushima, S.; Teranishi, K.; Hirai, S. Water Diffusion Measurement in Fuel-Cell SPE Membrane by NMR. *Energy* **2005**, *30*, 235–245.

(2) Molinero, V.; Goddard, W. Microscopic Mechanism of Water Diffusion in Glucose Glasses. *Phys Rev Lett* **2005**, *95*, 045701.

(3) Yang, C.; Xing, X.; Li, Z.; Zhang, S. A Comprehensive Review on Water Diffusion in Polymers Focusing on the Polymer-Metal Interface Combination. *Polymers* **2020**, *12*, 138.

(4) Le Bihan, D.; Iima, M. Diffusion Magnetic Resonance Imaging: What Water Tells Us About Biological Tissues. *PLoS Biol* **2015**, *13*, e1002203.

(5) Eisenberg, D.; Kauzmann, W. *The Structure and Properties of Water*; Oxford University Press: Oxford, UK, 2005.

(6) Rahman, A.; Stillinger, F. Molecular Dynamics Study of Liquid Water. *J Chem Phys* **1971**, *55*, 3336–3359.

(7) Laage, D.; Hynes, J. T. A Molecular Jump Mechanism of Water Reorientation. *Science* **2006**, *311*, 832–835.

(8) Laage, D.; Stirnemann, G.; Sterpone, F.; Rey, R.; Hynes, J. T. Reorientation and Allied Dynamics in Water and Aqueous Solutions. *Annu Rev Phys Chem* **2011**, *62*, 395–416.

(9) Chen, S. H.; Teixeira, J. Structure and Dynamics of Low-Temperature Water As Studied by Scattering Techniques. *Adv Chem Phys* **1986**, *64*, 1–45.

(10) Qvist, J.; Schober, H.; Halle, B. Structural Dynamics of Supercooled Water from Quasielastic Neutron Scattering and Molecular Simulations. *J Chem Phys* **2011**, *134*, 144508.

(11) Kikutsuji, T.; Kim, K.; Matubayasi, N. Diffusion Dynamics of Supercooled Water Modeled with the Cage-Jump Motion and Hydrogen-Bond Rearrangement. *J Chem Phys* **2019**, *150*, 204502.

(12) Sciortino, F.; Gallo, P.; Tartaglia, P.; Chen, S. H. Supercooled Water and the Kinetic Glass Transition. *Phys Rev E* **1996**, *54*, 6331–6343.

(13) Moilanen, D. E.; Wong, D.; Rosenfeld, D. E.; Fenn, E. E.; Fayer, M. D. Ion-Water Hydrogen-Bond Switching Observed with 2D IR Vibrational Echo Chemical Exchange Spectroscopy. *Proc Natl Acad Sci U S A* **2009**, *106*, 375–380.

(14) Ji, M.; Odelius, M.; Gaffney, K. J. Large Angular Jump Mechanism Observed for Hydrogen Bond Exchange in Aqueous Perchlorate Solution. *Science* **2010**, *328*, 1003–1005.

(15) Mukherjee, B. Microscopic Origin of Temporal Heterogeneities in Translational Dynamics of Liquid Water. *J Chem Phys* **2015**, *143*, 054503.

(16) Liu, C.; Zhang, Y.; Zhang, J.; Wang, J.; Li, W.; Wang, W. Interplay Between Translational Diffusion and Large-Amplitude Angular Jumps of Water Molecules. *J Chem Phys* **2018**, *148*, 184502.

(17) Vega, C.; Abascal, J. L. F. Simulating Water with Rigid Non-Polarizable Models: A General Perspective. *Phys Chem Chem Phys* **2011**, *13*, 19663–19688.

(18) Piskulich, Z.; Thompson, W. Examining the Role of Different Molecular Interactions on Activation Energies and Activation Volumes in Liquid Water. *J Chem Theory Comput* **2021**, *17*, 2659–2671.

(19) Berendsen, H. J. C.; Grigera, J. R.; Straatsma, T. P. The Missing Term in Effective Pair Potentials. *J Phys Chem* **1987**, *91*, 6269–6271.

(20) Laage, D.; Hynes, J. T. On the Molecular Mechanism of Water Reorientation. *J Phys Chem B* **2008**, *112*, 14230–14242.

(21) Montroll, E. W.; Weiss, G. H. Random Walks on Lattices. II. *J Math Phys* **1965**, *6*, 167.

(22) Dünweg, B.; Kremer, K. Molecular Dynamics Simulation of a Polymer Chain in Solution. *J Chem Phys* **1993**, *99*, 6983–6997.

(23) Yeh, I.-C.; Hummer, G. System-Size Dependence of Diffusion Coefficients and Viscosities from Molecular Dynamics Simulations with Periodic Boundary Conditions. *J Phys Chem B* **2004**, *108*, 15873–15879.

(24) Mills, R. Self-Diffusion in Normal and Heavy Water in the Range 1-45°. *J Phys Chem* **1973**, *77*, 685–688.

(25) Holz, M.; Heil, S. R.; Sacco, A. Temperature-Dependent Self-Diffusion Coefficients of Water and Six Selected Molecular Liquids for Calibration in Accurate 1H NMR PFG Measurements. *Phys Chem Chem Phys* **2000**, *2*, 4740–4742.

(26) Sciortino, F.; Geiger, A.; Stanley, H. E. Effect of Defects on Molecular Mobility in Liquid Water. *Nature* **1991**, *354*, 218–221.

(27) Chen, S. H.; Gallo, P.; Sciortino, F.; Tartaglia, P. Molecular-Dynamics Study of Incoherent Quasielastic Neutron-Scattering Spectra of Supercooled Water. *Phys Rev E* **1997**, *56*, 4231.

(28) Teixeira, J.; Bellissent-Funel, M. C.; Chen, S. H.; Dianoux, A. J. Experimental Determination of the Nature of Diffusive Motions of Water Molecules at Low Temperatures. *Phys Rev A* **1985**, *31*, 1913–1917.

(29) Tassaing, T.; Bellissent-Funel, M.-C. The Dynamics of Supercritical Water: A Quasielastic Incoherent Neutron Scattering Study. *J Chem Phys* **2000**, *113*, 3332–3337.

(30) Laage, D. Reinterpretation of the Liquid Water Quasi-Elastic Neutron Scattering Spectra Based on a Nondiffusive Jump Reorientation Mechanism. *J Phys Chem B* **2009**, *113*, 2684–2687.

(31) Noguere, G.; Scotta, J. P.; Xu, S.; Farhi, E.; Ollivier, J.; Calzavarra, Y.; Rols, S.; Koza, M.; Marquez Damian, J. I. Temperature-Dependent Dynamic Structure Factors for Liquid Water Inferred from Inelastic Neutron Scattering Measurements. *J Chem Phys* **2021**, *155*, 024502.

(32) Tolman, R. C. Statistical Mechanics Applied to Chemical Kinetics. *J Am Chem Soc* **1920**, *42*, 2506–2528.

(33) Piskulich, Z. A.; Mesele, O. O.; Thompson, W. H. Activation Energies and Beyond. *J Phys Chem A* **2019**, *123*, 7185–7194.

(34) Piskulich, Z.; Mesele, O.; Thompson, W. Removing the Barrier to the Calculation of Activation Energies: Diffusion Coefficients and Reorientation Times in Liquid Water. *J Chem Phys* **2017**, *147*, 134103.

(35) Mendis, C. H.; Piskulich, Z. A.; Thompson, W. H. Tests of the Stokes–Einstein Relation Through the Shear Viscosity Activation Energy of Water. *J Phys Chem B* **2019**, *123*, 5857–5865.

(36) Chen, S.-H.; Mallamace, F.; Mou, C.-Y.; Broccio, M.; Corsaro, C.; Faraone, A.; Liu, L. The Violation of the Stokes–Einstein Relation in Supercooled Water. *Proc Natl Acad Sci* **2006**, *103*, 12974–12978.

(37) Dueby, S.; Dubey, V.; Daschakraborty, S. Decoupling of Translational Diffusion from the Viscosity of Supercooled Water: Role of Translational Jump Diffusion. *J Phys Chem B* **2019**, *123*, 7178–7189.

(38) Guillaud, E.; Merabia, S.; de Ligny, D.; Joly, L. Decoupling of Viscosity and Relaxation Processes in Supercooled Water: A Molecular Dynamics Study with the TIP4P/2005f Model. *Phys Chem Chem Phys* **2017**, *19*, 2124–2130.

(39) Kincaid, J. F.; Eyring, H.; Stearn, A. E. The Theory of Absolute Reaction Rates and Its Application to Viscosity and Diffusion in the Liquid State. *Chem Rev* **1941**, *28*, 301–365.

(40) Stirnemann, G.; Wernersson, E.; Jungwirth, P.; Laage, D. Mechanisms of Acceleration and Retardation of Water Dynamics by Ions. *J Am Chem Soc* **2013**, *135*, 11824–11831.

(41) Paschek, D.; Geiger, A. Simulation Study on the Diffusive Motion in Deeply Supercooled Water. *J Phys Chem B* **1999**, *103*, 4139–4146.

(42) Faraone, A.; Liu, L.; Chen, S.-H. Model for the Translation–rotation Coupling of Molecular Motion in Water. *J Chem Phys* **2003**, *119*, 6302.

(43) Mazza, M.; Giovambattista, N.; Stanley, H.; Starr, F. Connection of Translational and Rotational Dynamical Heterogeneities with the Breakdown of the Stokes-Einstein and Stokes-Einstein-Debye Relations in Water. *Phys Rev E* **2007**, *76*, 031203.

(44) Bove, L. E.; Klotz, S.; Strässle, T.; Koza, M.; Teixeira, J.; Saitta, A. M. Translational and Rotational Diffusion in Water in the Gigapascal Range. *Phys Rev Lett* **2013**, *111*, 185901.

(45) Manogaran, D.; Subramanian, Y. Understanding Translational-Rotational Coupling in Liquid Water Through Changes in Mass Distribution. *J Phys Chem B* **2017**, *121*, 11344–11355.

(46) Stirnemann, G.; Laage, D. Communication: On the Origin of the Non-Arrhenius Behavior in Water Reorientation Dynamics. *J Chem Phys* **2012**, *137*, 031101.

(47) Piskulich, Z. A.; Laage, D.; Thompson, W. H. Activation Energies and the Extended Jump Model: How Temperature Affects Reorientation and Hydrogen-Bond Exchange Dynamics in Water. *J Chem Phys* **2020**, *153*, 074110.

(48) Qvist, J.; Mattea, C.; Sunde, E. P.; Halle, B. Rotational Dynamics in Supercooled Water from Nuclear Spin Relaxation and Molecular Simulations. *J Chem Phys* **2012**, *136*, 204505.

(49) Piskulich, Z. A.; Thompson, W. H. The Dynamics of Supercooled Water Can Be Predicted from Room Temperature Simulations. *J Chem Phys* **2020**, *152*, 074505.

(50) Rozmanov, D.; Kusalik, P. G. Transport Coefficients of the TIP4P-2005 Water Model. *J Chem Phys* **2012**, *136*, 044507.

(51) Kim, J. S.; Wu, Z.; Morrow, A. R.; Yethiraj, A.; Yethiraj, A. Self-Diffusion and Viscosity in Electrolyte Solutions. *J Phys Chem B* **2012**, *116*, 12007–12013.

(52) Laage, D.; Elsaesser, T.; Hynes, J. Water Dynamics in the Hydration Shells of Biomolecules. *Chem Rev* **2017**, *117*, 10694–10725.

Supplementary Information

Water Diffusion Proceeds via a Hydrogen-Bond Jump Exchange Mechanism

Axel Gomez,[†] Zeke A. Piskulich,[‡,¶] Ward H. Thompson,[*,‡] and Damien Laage[*,†]

[†]*PASTEUR, Department of Chemistry, École normale supérieure, PSL University, Sorbonne Université, CNRS, 75005 Paris, France*

[‡]*Department of Chemistry, University of Kansas, Lawrence, Kansas 66045, USA*

[¶]*Present address: Department of Chemistry, Boston University, Boston, MA 02215 USA*

E-mail: wthompson@ku.edu; damien.laage@ens.psl.eu

Simulation methodology

We performed classical molecular dynamics simulations on systems of 343 water molecules, described respectively with the SPC/E and TIP4P/2005 potentials and propagated with LAMMPS.[1] Each system is first equilibrated with a Nosé-Hoover thermostat at 298.15 K and a 100 fs relaxation time, and a Nosé-Hoover barostat at 1 atm and a 1000 fs relaxation time. The simulation box volume is then fixed at its average value (box side of 21.752204 Å for TIP4P/2005, and 21.725311 Å for SPC/E) and a 10 ns NVT trajectory is propagated with the velocity rescaling thermostat using a 100 fs relaxation time. A configuration is saved every 2 ns, leading to 5 independent configurations, which are then used as starting points for 5 independent 1 ns trajectories propagated in NVT with the same thermostat. These trajectories employ a 1 fs timestep, periodic boundary conditions with a 10.5 Å cutoff of Lennard-Jones interactions, an Ewald sum description of long-range electrostatic interactions with a 10^{-4} tolerance, and configurations are saved every 5 fs. Water molecules are kept rigid with the RATTLE algorithm. For the viscosity calculation, the 5 independent starting configurations are used to propagate 50 ns-long trajectories where only the pressure tensor is saved. For the calculation of activation energies, a 200 ns-long NVT trajectory is propagated, where configurations are saved every 1 ps. The resulting 200,000 independent configurations are used as starting points for 50 ps trajectories propagated in NVE.

H-bond jumps

H-bond jump times are determined from the jump tcf (Fig. S1). Jump times and their associated activation energies for the TIP4P/2005 and SPC/E water models have been calculated previously for the same system and in the same conditions, and we use the values reported in ref. 2.

The H-bond jump amplitude probability densities in Fig. 1d are well described by skew

normal distributions eq. S1 whose parameters are reported in Table S2.

$$4\pi\rho^2 p(\rho) = \frac{1}{\sigma\sqrt{2\pi}} \exp\left[-\frac{(\rho-\rho_0)^2}{2\sigma^2}\right]\left[1+\mathrm{erf}\left(\frac{\alpha\,(\rho-\rho_0)}{\sqrt{2}\sigma}\right)\right] \quad . \tag{S1}$$

Average displacements induced by a hydrogen-bond exchange

The local frame in which an H-bond jump occurs is defined for each jump at t_0 by the three O atoms involved: O^*, O_i and O_f. O^* is taken to be the origin of the local frame. The first frame vector $\vec{u}_1$ is defined along the $(O_iO^*O_f)$ angle bisector. The second one $\vec{u}_2$ is orthogonal to $\vec{u}_1$ and aligned with the vector connecting O_i to O_f in the plane formed by these three O atoms. The last vector $\vec{u}_3$ is orthogonal to both $\vec{u}_1$ and $\vec{u}_2$ and oriented to form a direct reference frame $\{\vec{u}_1, \vec{u}_2, \vec{u}_3\}$. The three vectors are then normalized. The average displacements of the atoms involved in the jump between $t_0 - 100$ fs and $t_0 + 100$ fs are given in Table S1. From this Table, we see that all atoms move in the plane formed by the three oxygen atoms and the displacements are reported graphically in Fig. 1a of the main text.

Table S1: Average displacement of the atoms directly involved in the H-bond exchange during the jump (Numbers between parentheses indicate uncertainties in the trailing digit).

	along $\vec{u}_1$ (Å)	along $\vec{u}_2$ (Å)	along $\vec{u}_3$ (Å)
O^*	-0.004(2)	0.415(2)	-0.000(2)
O_i	0.313(2)	-0.276(2)	0.0000(8)
O_f	-0.3090(9)	-0.2752(9)	0.000(2)
H^*	-0.007(1)	0.936(1)	0.000(2)

Diffusion of the $H_2O(H_2O)_4$ complex

To follow the long-time diffusion of a water molecule in absence of H-bond exchanges involving the H-bonds that it accepts or donates, we have employed the following set of restraints in order to prevent H-bond exchanges around O^* (but not transient breaks followed by the

reformation of the same H-bond): i) a soft half-harmonic potential on the O*-O distances to the four nearest neighbors, with a 5,000 kcal·mol^{-1}·nm^{-2} force constant that applies only beyond 3.33 Å, ii) a soft half-harmonic potential on O*-O distances to all water molecules which are not the four nearest neighbors, with a 5,000 kcal·mol^{-1}·nm^{-2} force constant that applies only below 3.33 Å, and iii) a strict half harmonic potential on the four H-bond angles involving O*, i.e. the two (HO*O) angles for the two H-bonds donated by O* and the two (HOO*) angles for the two H-bonds accepted by O*, with a 400 kcal·mol^{-1}·rad^{-2} force constant that applies only beyond 30°. These restraints were implemented in the LAMMPS simulations with the PLUMED library.[3,4] Figure S2 shows that the oxygen radial distribution function around O* is only marginally affected by these soft restraints.

Activation energy calculations

Following prior studies,[5–7] we employ the fluctuation theory for dynamics method to determine the activation energies from a single trajectory at 298.15 K.

For the diffusion coefficient obtained from the simulated msd, the activation energy has been shown[5,6] to be

$$E_a^{D^{pbc}_{MD}} = \lim_{t\to\infty} \frac{\langle \delta H(0)\,|\overrightarrow{r}(t) - \overrightarrow{r}(0)|^2\rangle}{\langle |\overrightarrow{r}(t) - \overrightarrow{r}(0)|^2\rangle} = \lim_{t\to\infty} \frac{\langle \Delta_H r^2(t)\rangle}{\langle \Delta r^2(t)\rangle}\ , \tag{S2}$$

where $\delta H(0) = H(0) - \langle H\rangle$ is the fluctuation in energy from its average value, and $\langle \Delta_H r^2(t)\rangle$ is the mean square displacement where each square displacement is weighted by the energy fluctuation.

The frame diffusion activation energy is calculated with eq. S2. The intact $H_2O(H_2O)_4$ cluster mean square displacement $\langle \Delta r^2(t)\rangle$ and mean-square displacement weighted by the energy fluctuations $\langle \Delta_H r^2(t)\rangle$ are shown in Fig. S3. Linear fits of $\langle \Delta r^2(t)\rangle$ and $\langle \Delta_H r^2(t)\rangle$ over the 10–50 ps interval are used to determine the long-time limit in eq. S2.

The pbc correction activation energy is determined from the viscosity activation energy[8]

(determined here from a numerical derivative, see below and Fig. S5), $E_a^{D_{corr}} = E_a^{1/\eta} + k_B T$.

The activation energy for the H-bond jump rate constant $1/\tau_{HB}$ is

$$E_a^{1/\tau_{HB}} = \tau_{HB} \int_0^\infty \mathrm{d}t \langle \delta H(0) p_i(0) p_f(t) \rangle \ . \tag{S3}$$

It has already been calculated by two of us and reported in ref. [2] for the SPC/E and TIP4P/2005 water models, and here we use the values determined in these prior studies.

The activation energy associated with the jump amplitude temperature dependence[7] is

$$E_a^{\langle \rho^2_{O^*,i,f} \rangle} = -\frac{1}{\langle \rho^2_{O^*,i,f} \rangle} \int_0^\infty \mathrm{d}\rho_{O^*,i,f} \ \frac{\partial p\left(\rho_{O^*,i,f}\right)}{\partial \beta} \ 4\pi \rho^4_{O^*,i,f} \ , \tag{S4}$$

and the reciprocal temperature derivative of the jump amplitude probability density is

$$4\pi \rho^2_{O^*,i,f} \ \frac{\partial p\left(\rho_{O^*,i,f}\right)}{\partial \beta} = -\frac{1}{N} \sum_{j=1}^{N} \delta H_j \delta \left[\rho^j_{O^*,i,f} - \rho_{O^*,i,f} \right] \ , \tag{S5}$$

where the sum runs over the N H-bond jump events collected during the simulation.

The computed activation energy values are reported in Table S3. Our model shows that the minor frame diffusion contribution, arising from water molecules which diffuse while keeping their H-bonds intact, exhibits a larger activation energy $E_a^{D^{pbc}_{frame}}$ than the H-bond exchange term $E_a^{D_{HB}}$. For water reorientation, the activation energy for the frame tumbling contribution had also been shown[7] to be larger (by $\sim$ 0.2 kcal/mol) than that for jump reorientation. Consequently, for both translation and reorientation dynamics in supercooled water, the more collective frame diffusion should become less and less important when the temperature decreases, and dynamics is expected to be increasingly due to H-bond exchanges directly involving the molecule that diffuses or rotates.

In addition, good agreement between the model and simulations is found when decomposing the activation energy into additive components. Following refs. [5–7], the instantaneous fluctuation in system energy is expressed as a sum of contributions arising

from the Lennard-Jones and Coulombic interaction energies as well as the kinetic energy: $\delta H = \delta KE + \delta V_{LJ} + \delta V_{Coul}$. In accordance with prior works[2,6] the results reported in Table S4 indicate that the diffusion activation energy is mostly determined by Coulombic interactions but also show that the jump model provides an excellent description of the activation energy decomposition.

Viscosity

The shear viscosity is calculated from the Green-Kubo equation involving the pressure tensor time-correlation function,

$$\eta = \frac{V}{k_B T} \int_0^\infty \langle P_{\alpha\beta}(0) P_{\alpha\beta}(t) \rangle \mathrm{d}t \ , \tag{S6}$$

where V is the simulation box volume and the $\langle P_{\alpha\beta}(0) P_{\alpha\beta}(t) \rangle$ correlation is averaged over the five correlations of the anisotropic stress tensor terms $P_{\alpha\beta}$[8] (Fig. S4).

Because of the very long simulations required to converge the viscosity activation energy with the fluctuation theory method,[8] here we determine the activation energy from an Arrhenius plot constructed from a series of six distinct simulations performed at 290, 295, 298.15, 300, 305 and 310 K using the same procedure as described above, with an initial NPT equilibration followed by a 10 ns NVT run from which 5 uncorrelated starting points are taken to propagate 5 independent 50 ns NVT trajectories. The resulting temperature dependence is shown in Fig. S5 for the TIP4P/2005 water model. The slope of the reciprocal viscosity along the reciprocal temperature is shown to be constant over this temperature range, which supports the validity of the activation energy determination from a finite difference around the ambient temperature.

Table S2: Parameters of the skew normal fits to the jump amplitude probability density distributions.

	ρ_0 (Å)	σ (Å)	α
O^*	0.402(3)	0.481(3)	2.16(3)
O_i	0.402(4)	0.508(4)	2.29(6)
O_f	0.402(4)	0.507(2)	2.30(4)

Table S3: Diffusion coefficients determined from our model eq. 4 with their respective contributions, from the simulated msd, and from experiments, and associated activation energies (Numbers between parentheses indicate uncertainties in the trailing digit).

	TIP4P/2005	SPC/E
τ_{HB} (ps)	3.657(7)[2]	3.160(3)[2]
$\langle\rho^2_{O^*}\rangle$ (Å^2)	0.675(3)	0.721(2)
$\langle\rho^2_{O_{i,f}}\rangle$ (Å^2)	0.722(2)	0.7464(9)
D_{HB} (10^{-5} cm^2/s)	1.273(4)	1.548(3)
D^{pbc}_{frame} (10^{-5} cm^2/s)	0.623(3)	0.749(5)
D_{corr} (10^{-5} cm^2/s)	0.335(3)	0.406(4)
D_{model} (10^{-5} cm^2/s)	2.232(6)	2.703(6)
D_{MD} (10^{-5} cm^2/s)	2.37(1)[2]	2.85(2)[2]
D_{NMR} (10^{-5} cm^2/s)	2.299[9,10]	
$E_a^{1/\tau_{HB}}$ (kcal/mol)	3.63(5)[2]	3.09(4)[2]
$E_a^{\langle\rho^2_{O^*}\rangle}$ (kcal/mol)	0.5(2)	0.40(6)
$E_a^{\langle\rho^2_{O_{i,f}}\rangle}$ (kcal/mol)	0.55(6)	0.51(4)
$E_a^{D_{HB}}$ (kcal/mol)	4.15(7)	3.55(5)
$E_a^{D^{pbc}_{frame}}$ (kcal/mol)	4.4(2)	3.9(3)
$E_a^{1/\eta}$ (kcal/mol)	3.7(4)	3.2(3)
$E_a^{D_{corr}}$ (kcal/mol)	4.3(4)	3.8(4)
$E_a^{D_{model}}$ (kcal/mol)	4.25(9)	3.68(9)
$E_a^{D^{pbc}_{MD}}$ (kcal/mol)	4.10(5)[2]	3.61(9)[2]
$E_a^{D_{NMR}}$ (kcal/mol)	4.2-4.4[9,10]	

Table S4: Decomposition of activation energies into kinetic energy, Lennard-Jones interaction energy and Coulombic interaction energy terms (in kcal/mol) (Numbers between parentheses indicate uncertainties in the trailing digit).

	$E_a^{1/\tau_{HB}}$	$E_a^{\langle\rho^2_{O^*}\rangle}$	$E_a^{\langle\rho^2_{O_{i,f}}\rangle}$	$E_a^{D_{HB}}$	$E_a^{D^{pbc}_{frame}}$	$E_a^{D_{corr}}$	$E_a^{D_{model}}$	$E_a^{D^{pbc}_{MD}}$
E_a	3.63(5)[2]	0.5(2)	0.55(6)	4.15(7)	4.4(2)	4.5(5)[8]	4.25(9)	4.10(5)[2]
KE	1.04(4)[2]	0.33(4)	0.36(3)	1.39(5)	1.2(1)	1.0(4)[8]	1.26(7)	1.16(4)[2]
LJ	-1.10(6)[2]	-0.16(7)	-0.24(4)	-1.30(8)	-1.2(2)	-0.8(2)[8]	-1.20(8)	-1.24(5)[2]
Coul	3.69(8)[2]	0.31(5)	0.43(7)	4.06(9)	4.5(3)	3.8(3)[8]	4.1(1)	4.18(6)[2]

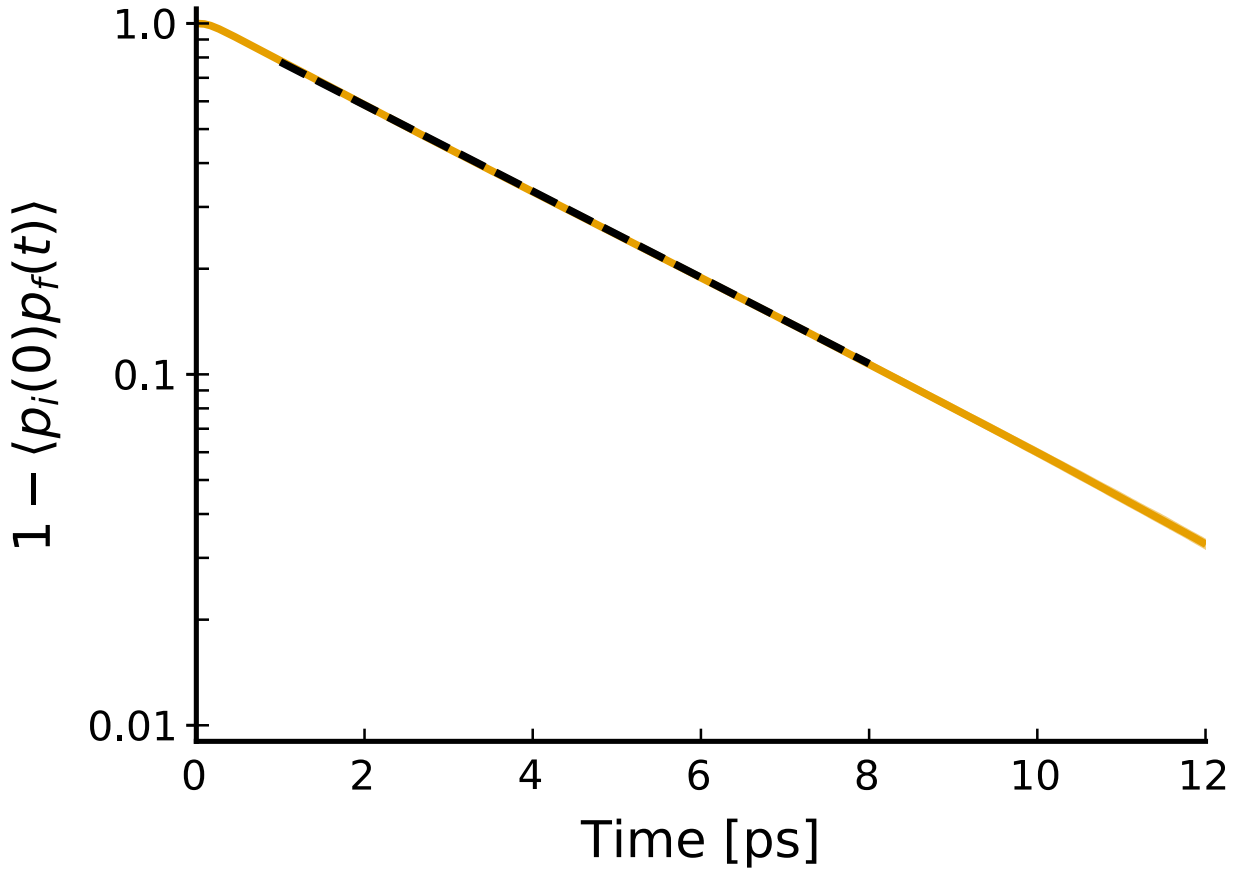

Figure S1: H-bond jump exchange time-correlation function $1 - \langle p_i(0) p_f(t) \rangle$ (orange) with the exponential fit (dashes) used to determine the jump time τ_{HB} determined from our TIP4P/2005 simulations.

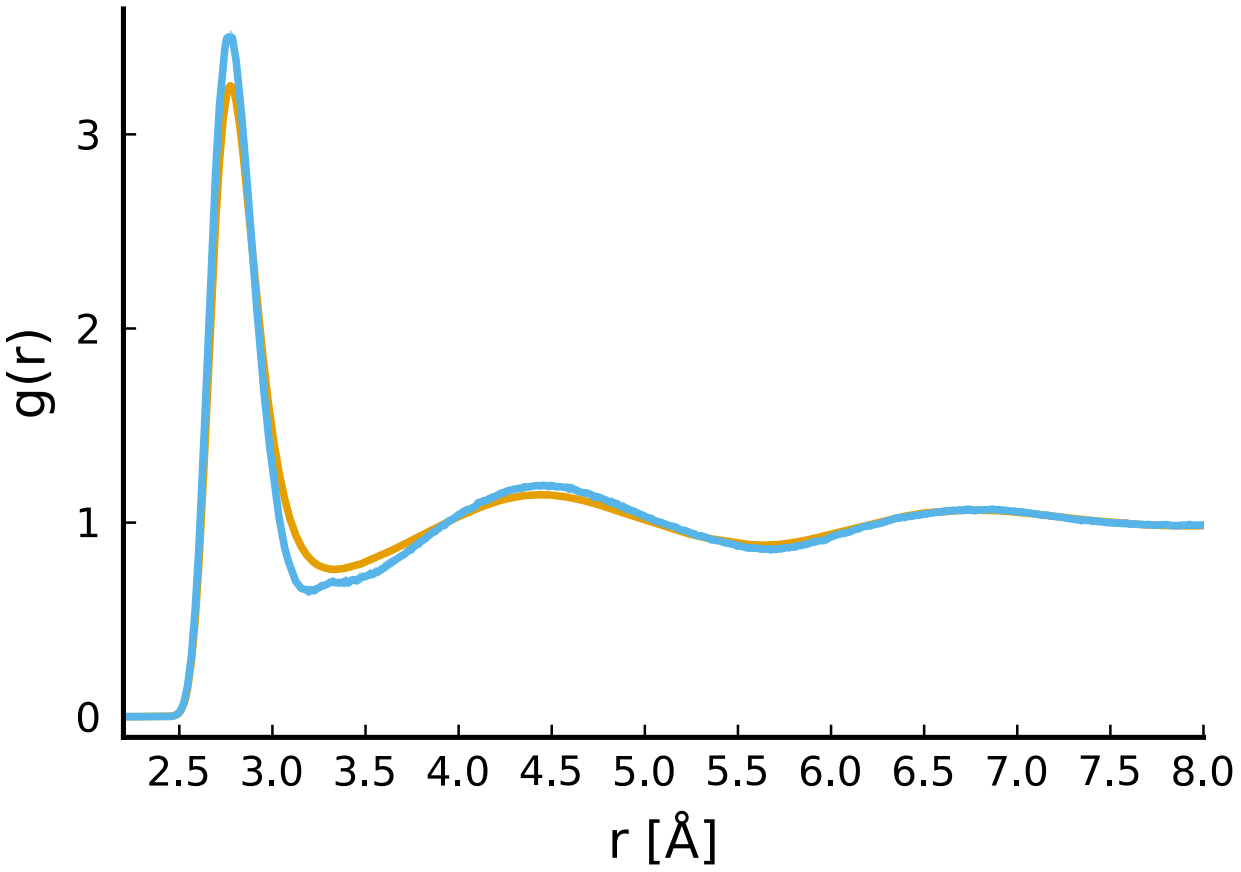

Figure S2: Oxygen radial distribution function around a water oxygen atom (orange) and around the O* oxygen atom in the $H_2O^*(H_2O)_4$ intact complex (blue), from our TIP4P/2005 simulations.

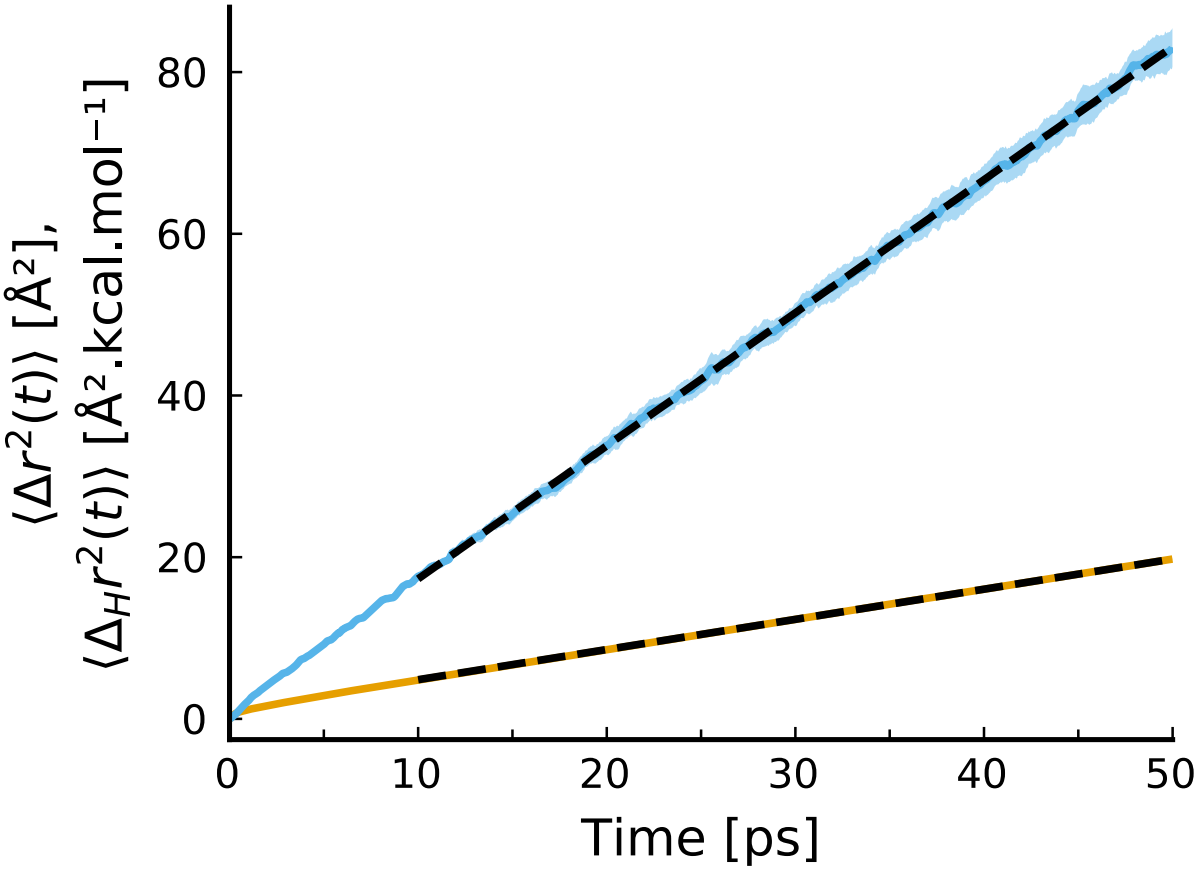

Figure S3: Intact $H_2O(H_2O)_4$ cluster mean square displacement $\langle \Delta r^2(t) \rangle$ (orange) and mean-square displacement weighted by the energy fluctuations $\langle \Delta_H r^2(t) \rangle$ (blue).

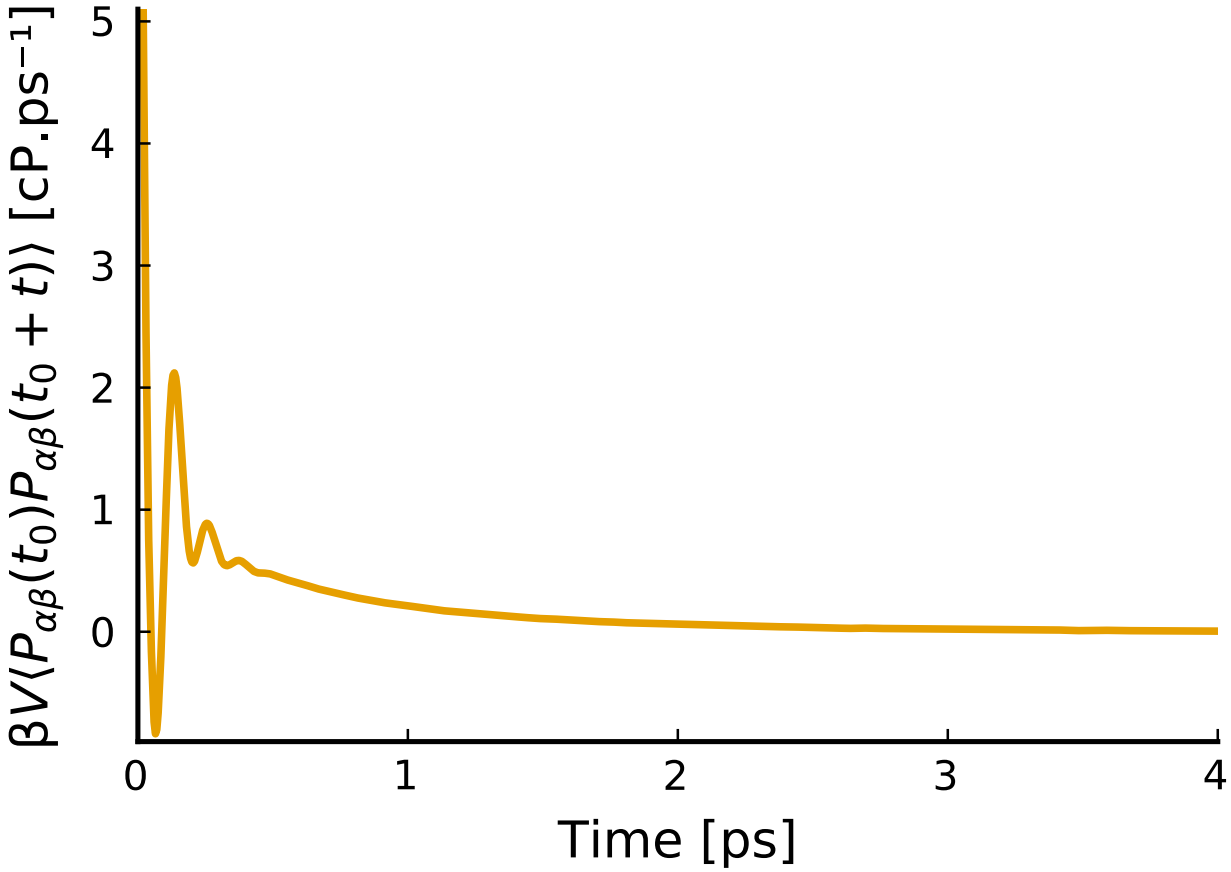

Figure S4: Pressure tensor time-correlation function $V/(k_BT)\langle P_{\alpha\beta}(0)P_{\alpha\beta}(t)\rangle$ calculated from our TIP4P/2005 simulations at 298.15 K.

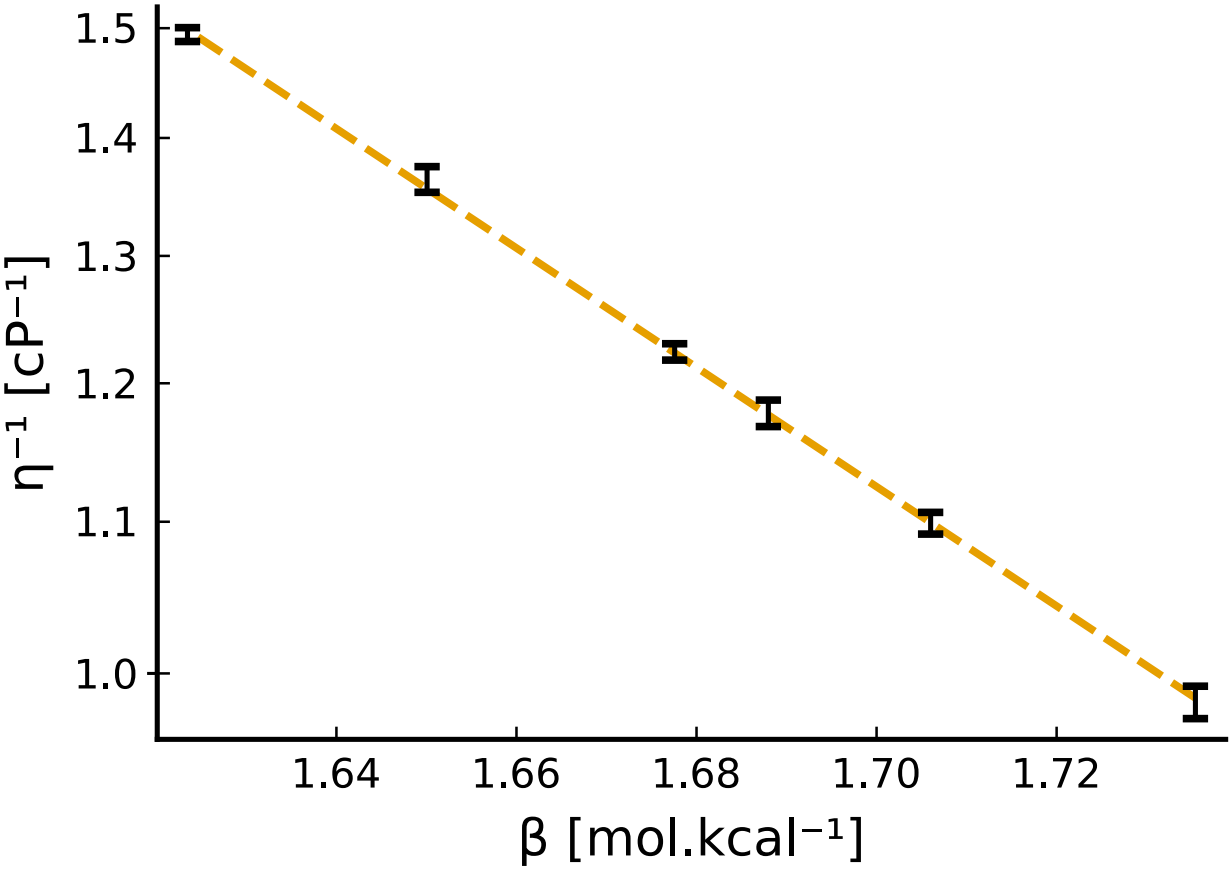

Figure S5: Arrhenius plot of the reciprocal viscosity $1/\eta$ along the reciprocal temperature $\beta = 1/k_B T$ for TIP4P/2005 simulations (black dots) with the fit used to determine the activation energy (orange dashes).

References

(1) Plimpton, S. Fast Parallel Algorithms for Short-Range Molecular Dynamics. *J Comp Phys* **1995**, *117*, 1–19.

(2) Piskulich, Z.; Thompson, W. Examining the Role of Different Molecular Interactions on Activation Energies and Activation Volumes in Liquid Water. *J Chem Theory Comput* **2021**, *17*, 2659–2671.

(3) PLUMED consortium, Promoting Transparency and Reproducibility in Enhanced Molecular Simulations. *Nat Methods* **2019**, *16*, 670–673.

(4) Tribello, G. A.; Bonomi, M.; Branduardi, D.; Camilloni, C.; Bussi, G. PLUMED 2: New Feathers for an Old Bird. *Comput Phys Commun* **2014**, *185*, 604–613.

(5) Piskulich, Z.; Mesele, O.; Thompson, W. Removing the Barrier to the Calculation of Activation Energies: Diffusion Coefficients and Reorientation Times in Liquid Water. *J Chem Phys* **2017**, *147*, 134103.

(6) Piskulich, Z. A.; Mesele, O. O.; Thompson, W. H. Activation Energies and Beyond. *J Phys Chem A* **2019**, *123*, 7185–7194.

(7) Piskulich, Z. A.; Laage, D.; Thompson, W. H. Activation Energies and the Extended Jump Model: How Temperature Affects Reorientation and Hydrogen-Bond Exchange Dynamics in Water. *J Chem Phys* **2020**, *153*, 074110.

(8) Mendis, C. H.; Piskulich, Z. A.; Thompson, W. H. Tests of the Stokes–Einstein Relation Through the Shear Viscosity Activation Energy of Water. *J Phys Chem B* **2019**, *123*, 5857–5865.

(9) Mills, R. Self-Diffusion in Normal and Heavy Water in the Range 1-45°. *J Phys Chem* **1973**, *77*, 685–688.

(10) Holz, M.; Heil, S. R.; Sacco, A. Temperature-Dependent Self-Diffusion Coefficients of Water and Six Selected Molecular Liquids for Calibration in Accurate 1H NMR PFG Measurements. *Phys Chem Chem Phys* **2000**, *2*, 4740–4742.